Kinetic Study of Oxidation of Cyclohexane Using Complex Catalyst

M. Jhansi L. Kishore and Anil Kumar
Dept. of Chemical Engineering, Indian Institute of Technology, Kanpur 208016, India

DOI 10.1002/aic.11173
Published online April 16, 2007 in Wiley InterScience (www.interscience.wiley.com).

With an effort to use a multimetallic catalyst system for oxidation of cyclohexane using oxygen, a binuclear monometallic macrocyclic ZrZr complex was prepared and covalently bonded to modified alumina support. The complex catalyst thus prepared was found to be thermally stable and was completely characterized by CHN, SEM-EDAX, TGA, and FTIR analysis. We carried out liquid phase oxidation of cyclohexane using molecular oxygen without any solvent, coreactant, or cocatalyst at considerably mild reaction conditions (150°C, 27 atm) with extremely high selectivity. The GC-MS of the liquid product formed showed the total conversion of as much as 19% having cyclohexanone and cyclohexanol in the ratio of 16:1. To explain the experimental data, a possible reaction mechanism has been proposed and rate constants (assuming single phase) at different temperatures were determined using an optimal curve fitting by applying genetic algorithm. We showed that the steady state approximation cannot be assumed, and for the pressure range studied (7–35 atm), the rate constants thus determined were found to be a function of temperature only. From experiments carried out at different temperatures, we found that for every rate constant, an Arrhenious type relation could be established. © 2007 American Institute of Chemical Engineers *AIChE J,* 53: 1550–1561, 2007

Keywords: heterogeneous catalysis, cyclohexane oxidation, bimetallic macrocyclic complex, reaction mechanism, rate constants

Introduction

The oxidation of cyclohexane is of great interest because it gives cyclohexanone, which is the key reactant in the production of adipic acid for production of nylon 66 and caprolactum for production of nylon 6.[1,2] The functionalization of unactivated C—H bonds of cyclohexane requires high pressure and temperature, and a number of catalysts have been developed. In this reaction, various oxidizing agents having active oxygen have been used such as peroxides (like hydrogen peroxide,[3,4] iodosobenzene,[5] *t*-butyl peroxide,[6] ozone[7]), solvents (such as heptanol, 2-methylpropanal, acetaldehyde), and cocatalysts[8] (such as acetic acid, chloroacetic acid, trifluoroacetic acid) have been used. The industrial processes employ catalytic and noncatalytic oxidation of cyclohexane.[9] Various catalysts have been developed and among them, cobalt (as acetate or palmitate) is the most commonly used catalyst with molecular oxygen as the oxidant, and the products formed are about equimolar mixture of cyclohexanol and cyclohexanone. Other catalyst systems using oxygen as oxidant such as iron and ruthenium catalyst,[8] nanostructured iron and cobalt catalyst,[10] immobilized cobalt catalyst,[11] polymer supported cobaltous palmitate,[12] and cobalt salen complex supported on silica[13] have been reported in the literature.

Very few data on kinetic rate constants have been reported in the literature. Several reactions have been proposed to explain various product formations in the oxidation of cyclohexane, but in all these, for determination of rate constants, only principal reactions (forming cyclohexanone and cyclohexanol) have been considered. There is only one study

Correspondence concerning this article should be addressed to A. Kumar at anilk@iitk.ac.in.

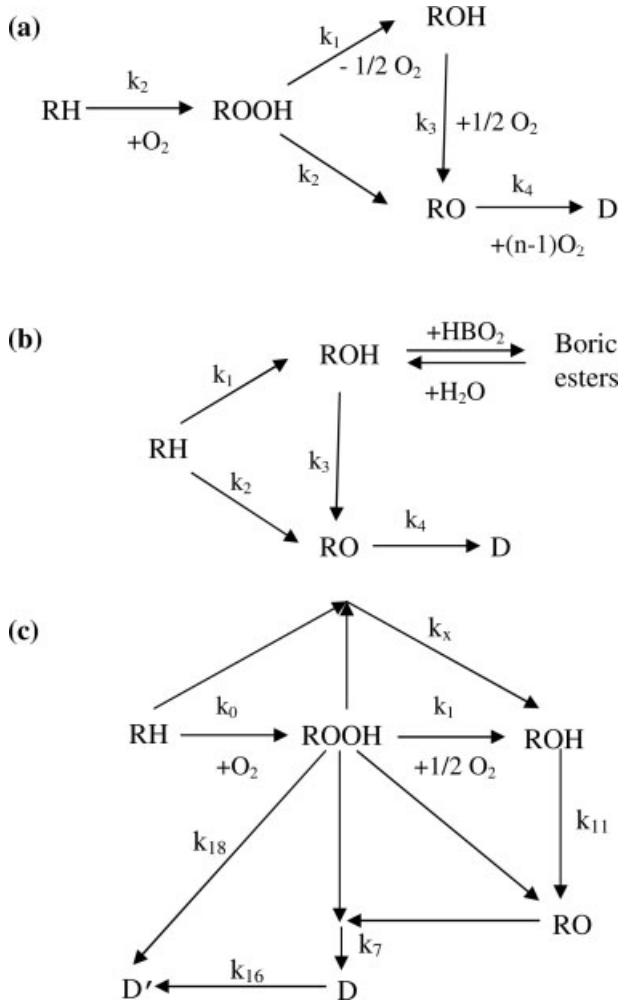

Figure 1. Literature kinetic models of cyclohexane oxidation showing the principal paths (formation of cyclohexanone (RO), cyclohexanol (ROH), and waste products (D).

reported on noncatalytic oxidation of cyclohexane,[9,14] where 154 elementary reactions were considered for the formation of principal products, and the rate constants for these reactions were calculated from statistical mechanical computations. The reported mechanisms for catalytic oxidation of cyclohexane consist of chain reaction involving hydroperoxy free-radical initiation, propagation, and termination steps. Literature reports three simplified kinetic models involving irreversible reaction steps, and two of these models have been utilized in data fitting.[15–17] In the first model (shown in Figure 1a), cyclohexane forms a hydroperoxide intermediate, which is then converted into cyclohexanone, cyclohexanol, and an unidentified product (D). In the second mechanism (shown in Figure 1b), the formation of intermediate is not considered, but further oxidation of cyclohexanol is terminated by the reaction with boric acid forming boric esters. Kharkova et al.[18] suggested an exhaustive model for noncatalytic oxidation based on experimental data reported in literature and estimated the rate constants and the concentration of the intermediate free radicals RO_2^*, RO*, R*, and OH*. Poherecki et al.[19] suggested a different catalytic model for cyclohexane oxidation as follows (shown in Figure 1c). Unlike earlier models, a lumped kinetic model having 10 irreversible rate constants was proposed and by assuming quasi-steady state approximation; concentrations of intermediate species were eliminated from the mathematical model. Using these reaction schemes, the determined rate constants were found to be dependent on species and catalyst concentration.

Moden et al.[20] reported the rate constants based on the redox properties of the active metal sites, where cyclohexyl hydroperoxide is an intermediate in cyclohexanol and cyclohexanone formation using O_2 as oxidant using MnAPO-5 catalyst. Loncarevic[21] studied the isothermal and nonisothermal oxidation of cyclohexane using polymer (copolymer of poly-4-vinylpyridine with divinylbenzene) supported catalysts with different contents of metal ions in the temperature range 110–170°C. The rate constants were obtained and were found to depend upon concentration of reacting species and the content of metal ions. Their dependence on the concentration of species was explained to arise from complex interactions between the reaction medium and the heterogeneous catalyst. Suresh[22–26] et al. reported cyclohexane oxidation and claimed[23] that the reaction medium consists of two phases (gas and liquid). They reported that the reaction was autocatalytic and zero order in oxygen, and a kinetic model was developed based on simplification of the accepted free radical scheme. They studied the interaction of kinetics and mass transfer, and showed that in an autocatalytic system, the dissolved oxygen level rises to saturation and falls as the rate of reaction increases.

Study of literature indicates the use of multimetallic catalysts to improve the catalytic efficiency and specificity, and this study is an effort in this direction. We further observed that using multimetallic catalysts, the heat of mixing (ΔH_m) for different salts determines the state of the metal on the support[27] (as ideal solution, solid solutions, ordered solution, mono or biphasic or surface alloys) and this way affecting the performance of the catalyst. The use of multimetallic complexes for catalysis is a step towards developing a system where ΔH_m has no role. Multimetallic complexes have been known in the early development of modern chemistry, and literature has mostly focused on their preparation and properties. These complexes are known to provide new reactivity patterns, because the interactions between the metals in these complexes help in promoting reaction as they will have greater oxidizing power. Some of the macrocyclic complexes used in catalyzing chemical reactions are given in Refs. 27–44, and these have been used as catalysts in chemical reactions. These reactions are mostly biological in nature for which temperatures needed are close to room temperature. Shulpin studied the oxidations of alkanes near room temperature using hydrogen peroxide catalyzed by monometallic transition metal complexes of vanadium, gold, and manganese,[45,46] which give their corresponding alcohols and ketones.

Unfortunately, the macrocyclic ZrZr complex is thermally unstable (breaks at 100°C determined by TGA) at high temperature. To overcome this problem, in this article, we have covalently bonded the complex to modified alumina, and as a result of this, the TG analysis shows that the thermal stability of the bound complex improves from 280°C (for the complex) to 580°C (of the final catalyst). We have studied the liquid phase oxidation of cyclohexane with this catalyst at different temper-

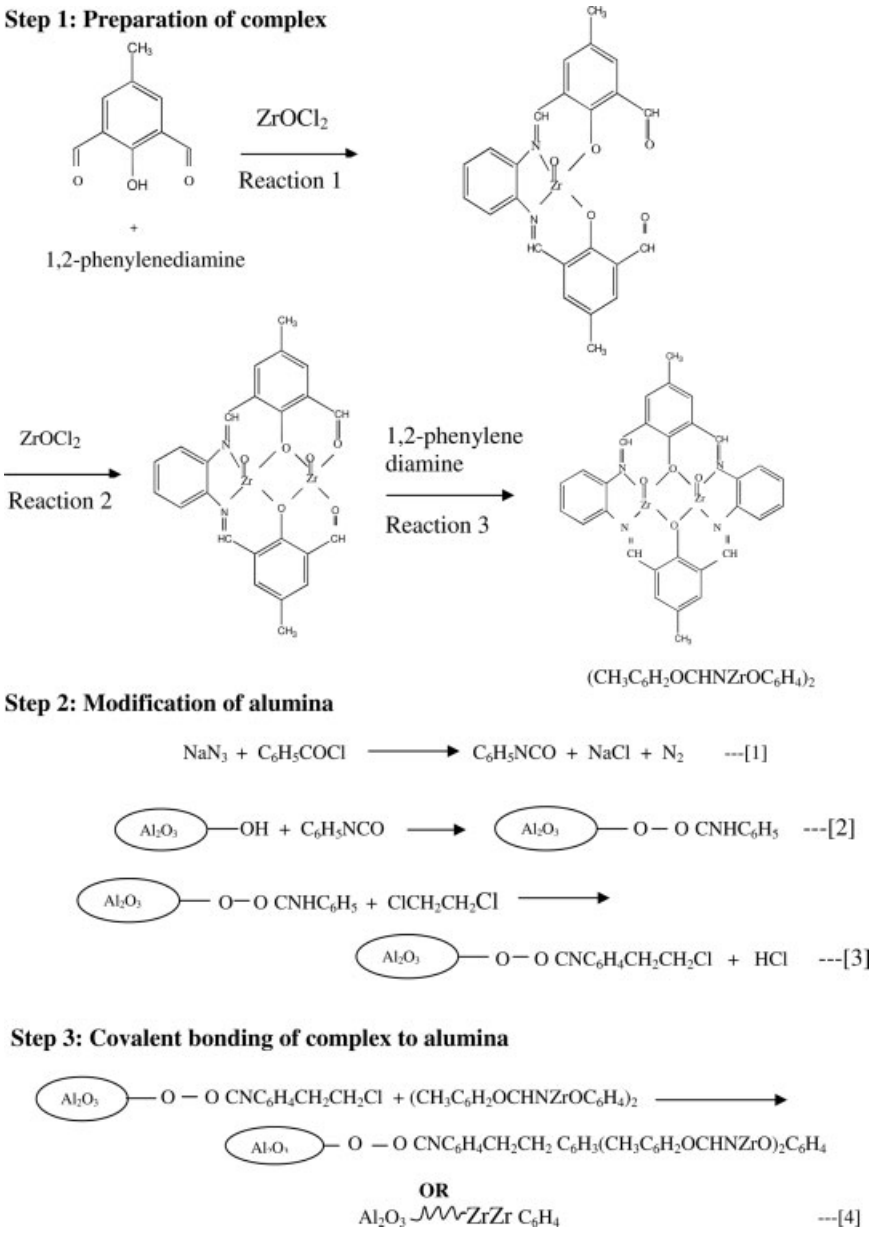

Figure 2. Steps of preparation of macrocyclic complex and the catalyst.

atures (125–225°C) and pressures (7–35 atm) and found that the major product formed for our catalyst was cyclohexanone with small amounts of cyclohexanol in the ratio (16:1). We have then proposed a new reaction mechanism and determined the rate constants by optimization of the concentrations of all the components of the reaction mixture. Our study shows that for the pressure range studied, the rate constants can be expressed in the usual Arrhenius form and are independent of the concentrations of the species in the reaction mass.

Experimental

Preparation of catalyst

Step 1: Preparation of Complex. The 2,6-diformyl-4-methylphenol needed for cyclic complexing agent is prepared following the procedure given in Ref. 47. The NMR spectrum of the dialdehyde that we prepared shows singlets at 11.42 (phenolic), 10.2 (aldehydic), 7.74 (aromatic), and 2.36 ppm (methyl) and is consistent with that of the assigned structure and matches with that given in Ref. 47. The reactions forming the cyclic complex with the zirconium are shown in step 1 of Figure 2 and the procedure of its preparation is given below.

Formation of ZrL′ in Reaction 1 of Step 1. To 50 ml of *N*,*N*-dimethylformamide at 313 K, 2,6-diformyl-4-methylphenol (0.95 g, 0.012) is added. 1,2-Phenylenediamine (0.65 g, 0.006 mol) is added to this solution. To this solution zirconium oxychloride (1.93 g, 0.006 mol) is added and the precipitate of ZrL′ complex formed is filtered, washed with diethyl ether, and dried. The FTIR spectrum shows the

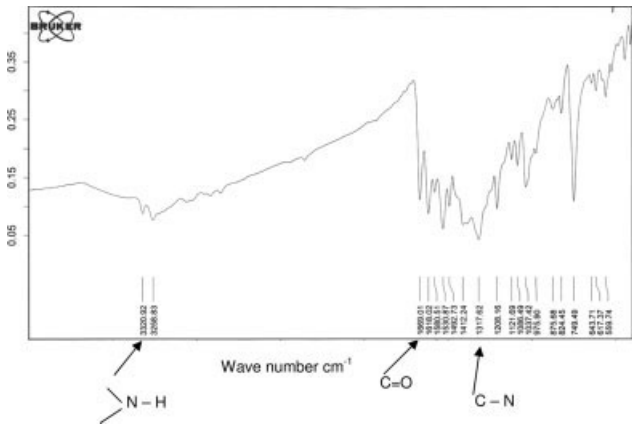

Figure 3. FTIR of the final ZrZr macrocyclic complex.

presence of functional groups C=N at 1690 cm^{-1} and C=O at 1614 cm^{-1} and C_6H_5—O at 1223 cm^{-1}.

Formation of ZrZrL′ in Reaction 2 of Step 1. The zirconium oxychloride (2.74 g, 0.008 mol) is dissolved in methanol (20 ml) at ambient temperature and ZrL′ (2.74 g, 0.008 mol) is added. The solution is stirred for 0.5 h and the crystals of the complex appear. These are collected by filtration and washed with diethyl ether and dried. The FTIR spectrum of this complex show C=O at 1618 cm^{-1} and C=N at 1508 cm^{-1} and C_6H_5—O at 1224 cm^{-1}.

Formation of ZrZrL in Reaction 2 of Step 1. The ZrZrL′ (2 g) is dissolved in 30 ml of methanol and 1,2-phenylenediamine (0.336 g) is added. The crystals that appear are collected by filtration and washed with diethyl ether and dried. The FTIR spectrum shows only C=N at 1512 cm^{-1} and no C=O peak appears as it forms C=N with 1,2-phenylenediamine (shown in Figure 3). The complex was characterized by the CHN and the EDAX analysis for elemental composition and TG analysis for thermal stability and discussed in the next section.

Step 2: Preparation of Modified Alumina. The alumina after drying at 773 K has been shown in Refs. 48 and 49 to have hydroxyl groups on its surface. Phenyl isocyanate is prepared according to Ref. 50 by reacting benzoyl chloride with sodium azide at 273 K in presence of benzene (Eq. 1, step 2 of Figure 2). The liquid and solid phases obtained are separated and the liquid formed, i.e., phenyl isocyanate (confirmed by matching its FTIR for the presence of N=C=O group) is reacted with the dried alumina for 4 h at ambient conditions (Eq. 2, step 2 of Figure 2). The FTIR spectrum shows —NH group at 3337 cm^{-1}, C=O at 1650 cm^{-1} and —OH at 3466 cm^{-1}. The carbamated alumina (3 g) is reacted with 50 ml of 1,2-dichloroethane in the presence of $ZnCl_2$ (5 mg) at 353 K for 2 h (Eq. 3, step 2 of Figure 2). The product is washed and dried and its FTIR spectrum shows carbamate group —CONH— at 2341 cm^{-1} and C—Cl at 694 cm^{-1}.

Step 3: Covalent Bonding of the Complex to Alumina. The complex prepared in step 1 is dissolved in methanol and reacted with the modified alumina at 333 K for 4–6 h in the presence of a Lewis acid catalyst $ZnCl_2$ (Eq. 4, step 3 of Figure 2).[51,52] The alumina catalyst thus obtained is washed and dried. The FTIR of the final catalyst shows the bonding of the complex at the Cl group, where the peak for C—Cl is disappeared.[53]

To confirm that the complex is indeed chemically bonded with the modified alumina, we have also carried out the similar bonding of the complex with small molecular weight compound like *t*-butanol. In the first step, phenyl isocyante is reacted with *t*-butanol. It's FTIR shows the phenyl group —CH— at 3035 cm^{-1} and aliphatic —CH_2— at 2940 cm^{-1}. In the next step, it is reacted with dichloroethane and its FTIR shows presence of -Cl at 780 cm^{-1}. The final step consists of binding the complex with the carbamated *t*-butanol compound. The FTIR of the final product shows the reduction of the intensity of the peak corresponding to the Cl group, this way suggesting that the ZrZr complex is attached to the carbamate modified *t*-butanol.

Reaction studies

Oxidation of cyclohexane has been studied in a batch reactor made of stainless steel of 500 ml volume. The reactor is provided with an inlet for introducing gas and collecting the sample, a pressure gauge to monitor the pressure in the reactor, a thermocouple to measure the temperature inside the reactor, and a furnace to heat the reactor to required temperature. The temperature is maintained using an on–off controller. Cyclohexane is fed into the reactor along with 1 g of catalyst. The reactor is then closed and oxygen is filled in the reactor at a pressure of 7 atm. The reactions have been carried out and the variation of conversion is measured at different reaction times (1–8 h) and temperatures (125–225°C).

Characterization of the catalyst

We have characterized the catalyst prepared for thermal stability, surface area, metal leaching ability, presence of acidic sites, and measured its catalytic ability for the oxidation of cyclohexane using molecular oxygen. The surface area is measured on a Coulter SA2100 instrument and is analyzed by the BET method. The TPD measurements are made on a micromeritrics Pulse ChemiSorb 2705 instrument. The complex prepared is characterized by FTIR spectroscopy and its composition has been confirmed by CHN analysis and SEM–EDAX analysis. The products obtained after reaction were analyzed by gas chromatography (GC) using a fused silica capillary column 0.25 mm × 50 m film thickness 0.25 μm with flame ionization detector, and the gas chromatography mass spectroscopy (GC-MS) was carried out using a Shimadzu QP-2000 instrument.

Results and Discussion

Characterization of the complex

We have already given the IR of the complex (shown in Figure 3) at different stages of its preparation confirming the formation of complex in the "Preparation of catalyst" section. It shows the C=N at 1512 cm^{-1} which is seen in the structure of the ZrZr complex of step 1 of Figure 2. The complex exists as $ZrZrL(OCl_2)_2$, where L is the ligand $((CH_3C_6H_2OCHNC_6H_4)_2)$ and OCl_2 is present because the Zirconium oxychloride has been used as metal salt during the complexation. The theoretical values of C, H, and N are calculated from the above structure and compared with ex-

Table 1. CHN and SEM-EDAX Analysis of the Complex and the Catalyst

	Complex			Catalyst
	Theoretical	Experimental	SEM-EDAX	SEM-EDAX
C	43.31	42.57	44.65	–
H	5.3	3.72	–	–
N	10.4	7.13	8.71	–
Zr	9.68	–	7.04	2.25

perimental values given in Table 1. In view of the above, the SEM–EDAX analysis of the complex has been carried out by coating it with gold under vacuum to make the sample conducting for electrons. The EDAX analysis gave C and N values and is also reported in the same table. The difference between the theoretical and experimental values is less then 5% and lies within the experimental error.

We have also tried to prepare a single crystal of the complex to obtain its structure by X-ray diffraction analysis. We used the evaporation technique using methanol and dimethyl formamide as solvents, solvent–nonsolvent diffusion technique using methanol, and *n*-hexane and vapor diffusion technique using methanol and diethyl ether. Single crystals however could not be prepared due to low solubility of the complex and leaving a few unfilled cavities with in a given complex cannot be totally ruled out.

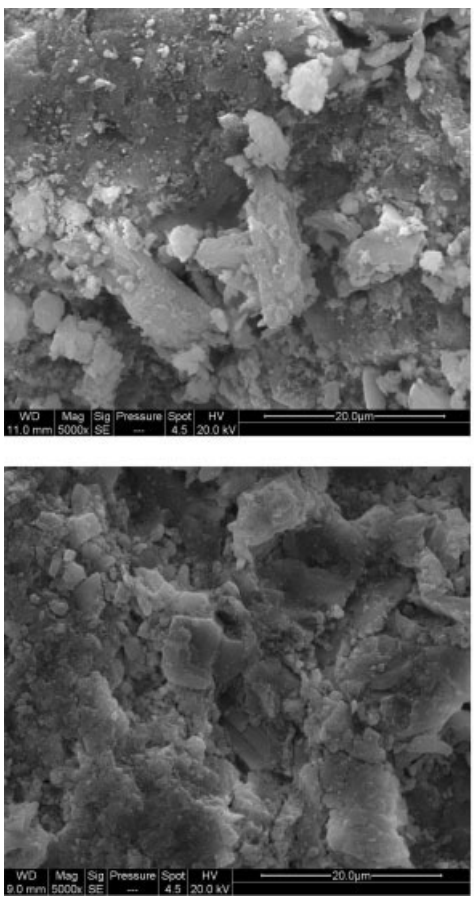

Figure 4. SEM photographs of the complex catalyst.

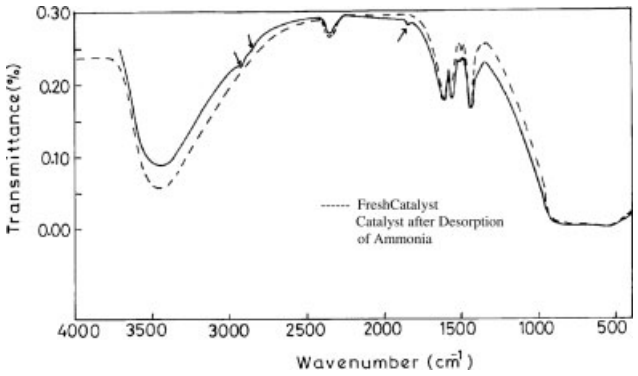

Figure 5. FTIR of the catalyst before and after saturation with ammonia: the arrows above show the active sites on the catalyst surface.

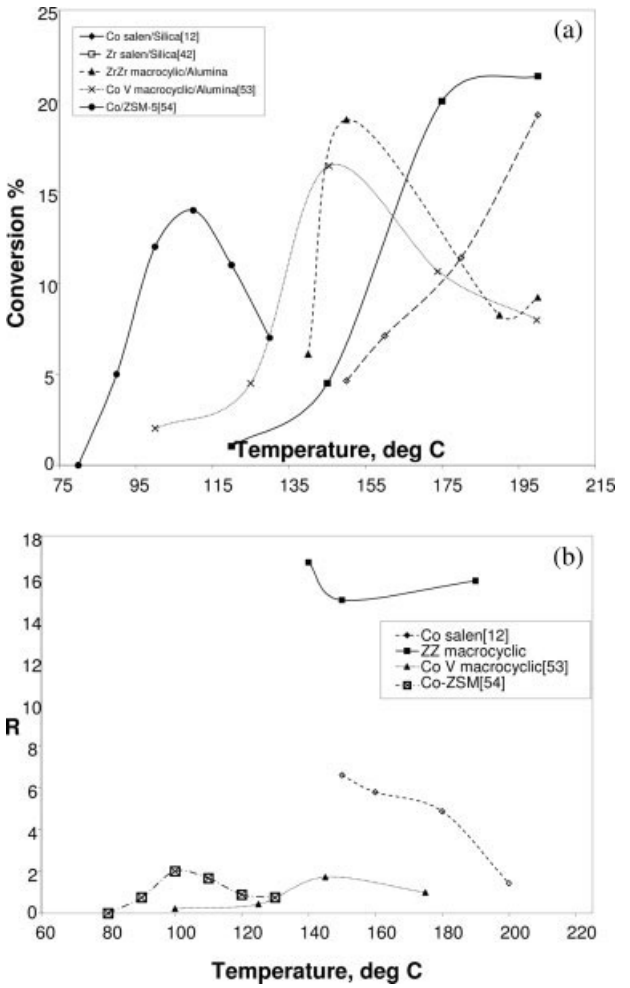

Figure 6. (a) Various catalysts used for cyclohexane oxidation and its effect upon conversion of cyclohexane for 8 h of reaction time; (b) ratio of cyclohexanone to cyclohexanol for various catalysts used for cyclohexane oxidation for 8 h of reaction time.

For CoV/alumina[53] and Co/ZSM-5[54] catalysts, the ratio is close to 1. For Zr/Silica catalyst,[42] the products obtained were cyclohexanol and cyclohexene and cannot be shown in this figure.

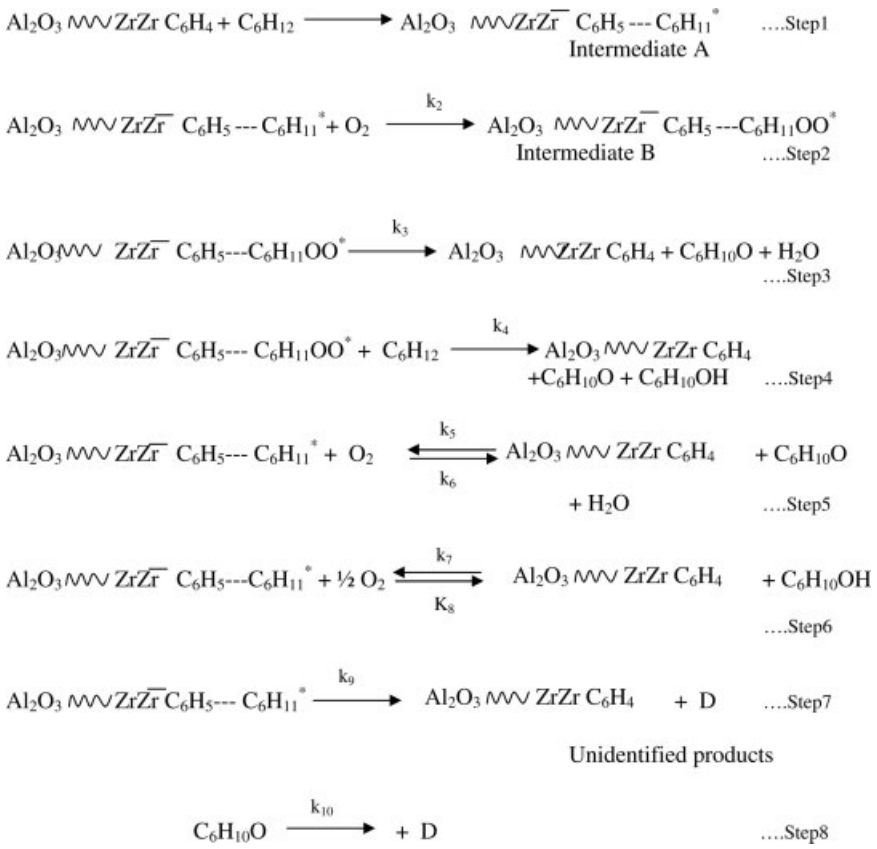

Figure 7. A plausible mechanism of oxidation of cyclohexane using homonuclear macrocyclic zirconium complex bound to carbamted alumina.

Characterization of the catalyst

The loading of the complex on the support has been confirmed by the FTIR of the catalyst as discussed in the "Reaction Studies" section. The SEM-EDAX analysis of the final catalyst has also shown the presence of Zirconium on the catalyst (given in Table 1). The SEM micrographs of the catalyst before and after the reaction are shown in Figure 4. The surface area of unmodified alumina and the catalyst (fresh as well as used) was calculated using the BET method. The surface area of unmodified alumina was 226.45 m^2/g, and after loading the complex it reduced to 138.9 m^2/g (a decrease of about 38%). The surface area of the catalyst further decreased to 75 m^2/g for 10-h reaction and does not change after further usage.

The thermal stability of the catalyst has been determined by thermogravimetric analysis. About 10–15 mg of the complex and the complex catalyst is taken and the weight loss is measured in the temperature range of 323–1253 K in an inert atmosphere. The complex was found to be stable upto 553 K and the complex catalyst was stable upto 853 K. This shows that upon bonding the complex to the support, the stability increased and as a result of this, the complex catalyst can now be used for high temperature reactions.

We have carried out the TPD of the final catalyst to study the acidic properties of the catalyst. The catalyst (60 mg) is first pretreated at 373 K to remove the moisture present in it and it is subsequently saturated with 2.5 ml ammonia at room temperature. The desorption is carried out up to 1223 K and the TPD curve showed one peak at 445 K. The catalyst was found to be stable upto 523 K and no further response has been observed after that temperature. FTIR of the catalyst before and after ammonia desorption had been taken and shown in Figure 5, and the additional peaks observed have been marked, which indicate the presence of acid sites.

Catalytic Study. Oxidation of cyclohexane with binuclear monometallic macrocyclic ZrZr complex catalyst supported on alumina has been studied between 125–225°C, pressure range of 7–35 atm of O_2, and a residence time of 2–8 h. This range of temperature was chosen because the percent cyclohexanone formed beyond this range was very small (less than 1%). The liquid products obtained have been analyzed by the GCMS and the peaks have been identified as cyclohexane (residence time: 7.1 min), cyclohexanone (residence time: 13.7 min), and cyclohexanol (residence time: 8.9 min). An overall conversion of 19% of cyclohexane is found to occur at 423 K for 8 h of reaction time. The major product obtained is cyclohexanone (about 11%), whereas very small amount of cyclohexanol (about 0.8%) has been formed. As the reaction time is increased from 2 to 8 h, the conversion increased from 2% to 19%. The yield of cyclohexanone increased from 1% to 11%, whereas its selectivity was 25% for 4 h of reaction, and 58% for 6 h whereas for 8 h the selectivity decreased to 50%. The decrease in cyclohexanone selectivity suggests that after 6 h of reaction time, cyclohexa-

Table 2. Conversion, Yield, and Selectivity of Cyclohexane, Cyclohexanol, and Cyclohexanone Obtained Using ZrZr/Alumina at Different Temperatures with the Initial Oxygen Pressure of 7 atm

Temperature, K	Time, min	Cyclohexane Conversion, %	Cyclohexanone Yield, %	Cyclohexanol Yield, %	Cyclohexanone Selectivity, %	Cyclohexanol Selectivity, %
473	0	0	0	0	0.00	0.00
	30	0.958	0.219	0	22.86	0.00
	60	1.602	1.123	0	70.10	0.00
	90	8.194	3.002	0.012	36.64	0.15
	120	7.816	5.33	0.038	68.19	0.49
	150	7.33	5.88	0.179	80.22	2.44
	180	8.93	5.51	0.259	61.70	2.90
	210	7.02	6.81	0.311	97.01	4.43
	270	7.7	5.74	0.346	74.94	4.49
	300	9.22	5.77	0.364	62.58	3.95
	330	8.14	5.82	0.337	71.50	4.14
	360	7.63	5.77	0.364	75.62	4.77
	480	7.6	5.45	0.315	71.71	4.14
463	0	0	0	0	0	0
	30	3.891	3.495	0.063	89.82	1.62
	60	5.272	3.794	0.111	71.97	2.11
	90	4.111	6.626	0.137	161.18	3.33
	120	4.451	3.952	0.172	88.79	3.86
	150	4.555	4.153	0.189	91.17	4.15
	180	5.348	3.633	0.199	38.55	2.11
	210	3.853	3.389	0.187	87.96	4.85
	270	3.903	3.498	0.195	89.62	5.00
	300	4.019	3.57	0.203	88.83	5.05
	330	4.248	3.04	0.402	65.73	9.46
	360	8.25	3.912	0.262	47.41	3.17
	480	4.325	3.657	0.228	84.55	5.27
443	0	0	0	0	0	0
	30	5.318	4.887	0	91.90	0.00
	60	3.478	3.006	0	86.43	0.00
	90	3.922	3.335	0.108	85.03	2.75
	120	3.729	3.168	0.117	84.96	3.14
	150	3.668	3.122	0.131	85.11	3.57
	180	4.257	3.547	0.171	83.32	4.02
	210	5.491	3.587	0.19	65.21	3.46
	210	5.324	4.41	0.133	82.83	3.02
	270	5.349	6.03	0.274	112.73	2.50
	300	7.826	4.535	0.238	57.95	5.12
	330	6.189	3.52	0.243	56.88	3.04
	360	10.609	5.65	0.355	53.26	3.93
	480	18.98	11.126	0.384	58.6195	2.00
413	0	0	0	0	0	0
	30	1.8	1.54	0.00	85.56	0
	60	2.5	1.94	0.00	77.60	0
	90	5.2	4.50	0.011	86.54	0.21
	120	4.9	4.25	0.024	86.73	0.49
	150	5.9	4.75	0.036	80.51	0.61
	180	5	4.66	0.66	93.20	13.20
	210	5	4.53	0.780	90.60	15.60
	270	4.9	4.51	0.107	92.04	2.18
	300	4.8	4.44	0.114	92.50	2.38
	330	6.1	4.26	0.094	69.86	1.54
	360	5.1	4.61	0.137	90.39	2.69
	480	4.4	3.82	0.152	86.82	3.45

$$\%\,\text{Conversion} = 1 - \frac{\text{Number of moles of the reactant in the product}}{\text{Total number of moles of the reactant in the feed}} \times 100.$$

$$\%\,\text{Yield} = \frac{\text{Number of moles of a particular component in the product}}{\text{Total number of moles of the reactant in the feed}} \times 100.$$

$$\%\,\text{Selectivity} = \frac{\text{Number of moles of a particular component in the product}}{\text{Total number of moles of the reactant in the feed}} \times 100.$$

none has converted to other products. As far as cyclohexanol is concerned, the amount of cyclohexanol formed at 423 K for 8 h of reaction was the highest and at that condition, and the yield was 0.8% with a selectivity of 20%.

The effect of temperature and oxygen pressure (7–35 atm) on cyclohexane oxidation for 8 h of reaction has been studied in the range of 398–498 K and the optimum results were obtained at 423 K. For temperatures above this, the conversion is

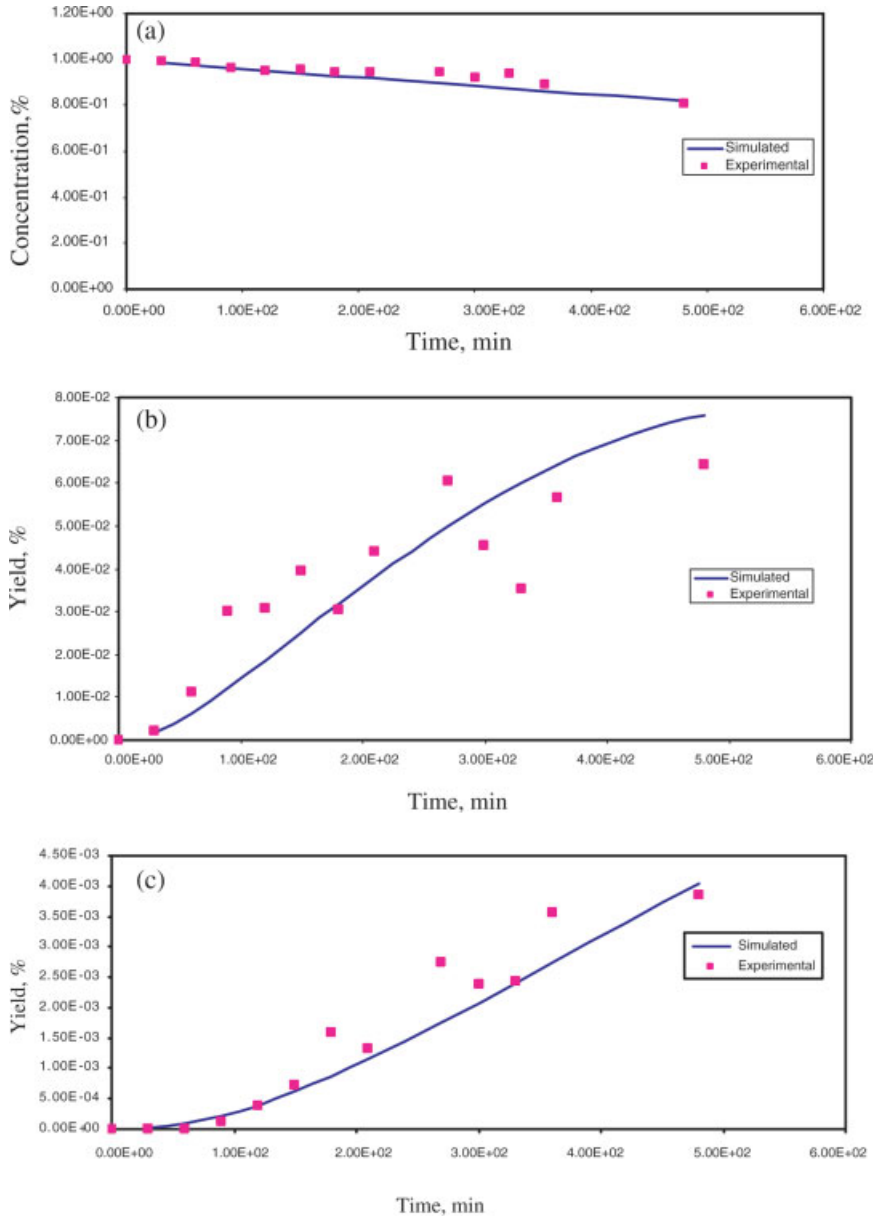

Figure 8. (a) Curve fitting of concentration of cyclohexane versus time using genetic algorithm for 8 h of reaction at 150°C using ZrZr/Alumina; (b) curve fitting of yield of cyclohexanone versus time for 8 h of reaction at 50°C using ZrZr/alumina; (c) curve fitting yield of cyclohexanol versus time for 8 h of reaction at 150°C using ZrZr/alumina; (d) concentration of intermediate A time for 8 h of reaction at 150°C using ZrZr/alumina; (e) concentration of intermediate B versus time for 8 h of reaction at 150°C using ZrZr/alumina; (f) concentration of D (unidentified products) versus time for 8 h of reaction at 150°C using ZrZr/alumina.

[Color figure can be viewed in the online issue, which is available at www.interscience.wiley.com.]

found to decrease and the yield and selectivities of the products also varied following the same trend. A plausible explanation for the fall in conversion could be found in the mechanism of reaction of cyclohexane in presence of the catalyst, as will be discussed later.

Comparison of our work with literature

In our earlier works, we had prepared cobalt salen[12] complex catalyst covalently bonded on silica support. We carried out oxidation of the cyclohexane at similar reaction conditions with molecular oxygen as the oxidizing agent. The major product was cyclohexanol whereas cyclohexanone and cyclohexene were formed in smaller quantity. However, for the present catalyst, the cyclohexanone was formed with higher selectivity. Figure 6 shows the comparison of the oxidation of cyclohexane studied in our laboratory using salen and macrocyclic complexes. Figure 6a shows the effect of temperature on cyclohexane conversion at 8 h residence time for different catalysts. For salen complex catalysts (Zr/

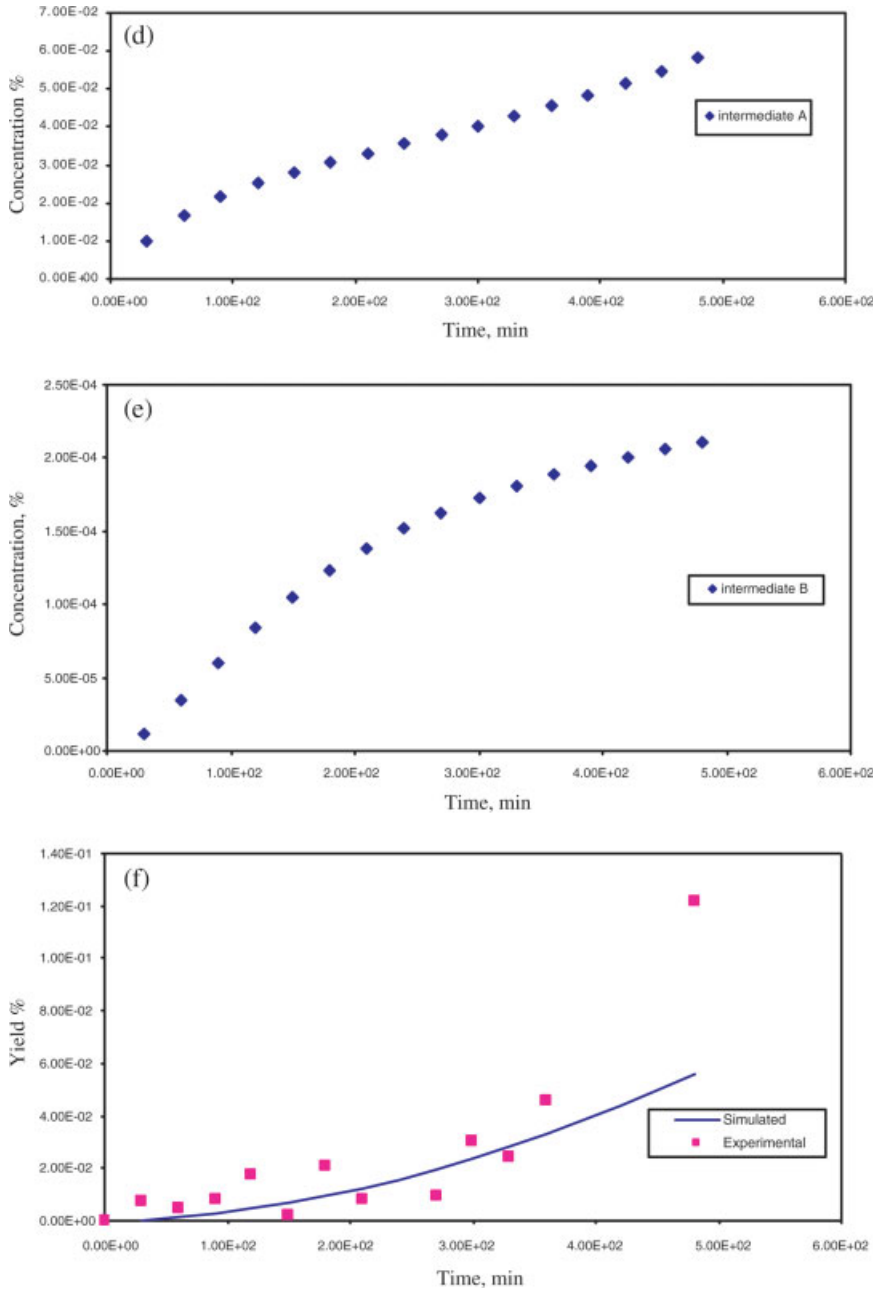

Figure 8. (*Continued*)

Silica[43] and Co/Silica[12]), the conversion at 8 h of reaction increases with temperature, whereas for the macrocyclic complex catalysts (ZrZr/Alumina and CoV/Alumina[54]) and Co/ZSM-5 catalyst,[55] the conversion starts to decrease after a particular temperature. The explanation of this observation is inherent in the fact that the steady state approximation is not valid, and various reaction parameters interact to give reduced intermediate concentration and hence conversion. This is explained in the "Determination of rate constants" section mathematically. Further it may be observed from this figure that most of the catalysts give a final conversion of around 20%, with an exception to mesoporous Ce-MCM-41[56] catalyst, for which the conversion is 95%. However, since the oxidizing agent is hydrogen peroxide, and not oxygen, we have not shown their result in this figure.

In Figure 6b, we have plotted the ratio (R = [cyclohexanone]/[cyclohexanol]) of cyclohexanone to cyclohexanol after 8 h of reaction time as a function of temperature. We notice that Co/ZSM-5 and CoV/Alumina catalyst give the value of R close to unity. The Co/Silica gives a decreasing ratio with increasing temperature, and the value of R falls in the range of 6–1. As opposed to this, in Zr/Silica catalyst, there was no formation of cyclohexanone, and only cyclohexanol and cyclohexene were formed and these results cannot be shown in this figure. The ZrZr/Alumina catalyst has the highest ratio of around 16.

Proposed reaction mechanism

Several reaction mechanisms have been proposed to explain the role of the catalyst and the kind of products that are formed, but for model fitting of experimental data, only, principal pathways (formation of cyclohexanone and cyclohexanol) are considered for the global kinetics of the oxidation. We have followed the model suggested by Pohorecki et al. (Figure 1c) and defined rate constants based on this mechanism in which some reactions are taken as reversible. All the reported literature shows that cyclohexanone and cyclohexanol are formed in almost equimolar quantities, whereas in our case, the selectivity for cyclohexanone is considerably more than the former. The usual mechanism suggests the formation of cyclohexylperoxy radical (intermediate), which is then converted into cyclohexanol. To show that this intermediate is not formed in our case, we added triphenyl phosphine to the reaction mass, which converts the peroxy radical into cyclohexanol. The GC of the sample shows that the concentration of cyclohexanol remains unchanged, which goes to confirm that these are not present in the reaction mass.

Zirconium metal in catalysis has been mostly used to give an acidic property and there are only very few examples in which zirconium directly has been used as a catalyst. Among these reactions involving zirconium, the most quoted is the sulfated zirconia, which has been used for reforming of C_6 hydrocarbons.[57] In this, the sulfate group serves to generate ionic radical and through the disproportionate reaction produce cyclohexane through cyclization. These ionic radical species can also polymerize, and this way it may give the catalyst deactivation. In the reported experimentation, the formation of cyclopentane was similarly explained. Based on this mechanism, in the oxidation of cyclohexane using heterobinuclear macrocyclic Co-V complex catalyst,[54] we have proposed a cationic radical intermediate in which cationic radicals are formed through an electron abstraction from the catalyst, which can add on an oxygen molecule to it. This new oxygenated intermediate involving the catalyst forms cyclohexanol by oxygen transformation.

In our catalyst, the potential site for the oxidation reaction to take place can be either ligand centered or metal centered.[58] Observing that in our experiments cyclohexanone is formed in considerably larger amount, to explain our result we have similarly proposed that the reaction could have occured at the complex site (Figure 7). The cyclohexane molecule first forms a carbonium ion intermediate-A (step 1 of Figure 7) and donates an electron to the complex site,[59] thus forming a reactive radical cation. Intermediate-A can react with oxygen molecule forming an intermediate-B with the catalyst (step 2 of Figure 7), which forms cyclohexanone as shown in step 3 of Figure 7. This also can react with another molecule of cyclohexane forming cyclohexanone and cyclohexanol (step 4 of Figure 7). In step 5 of Figure 7, intermediate A is shown to react with oxygen forming cyclohexanone, and in step 6 cyclohexanol is formed through a reversible reaction. Unidentified side products (D) are also formed from intermediate A (step 7 of Figure 7) and cyclohexanone (step 8 of Figure 7). The decrease in cyclohexanone selectivity with time can be explained by the formation of unidentified product (D) and the reverse formation of carbonium ion in step 5.

Determination of rate constants

Following the reaction mechanism given in Figure 7, we can write mole balance equations for each component of the reaction as shown below:

$$d[C_6H_{12}]/dt = -k_1[C_6H_{12}] - k_4[C_6H_{12}][C_6H_{11}OO^*] \quad (1)$$

$$d[C_6H_{11}^*]/dt = k_1[C_6H_{12}] - (2k_5 + k_2 + k_7)[C_6H_{11}^*][O_2] + k_6[C_6H_{10}O] + k_8[C_6H_{10}OH] \quad (2)$$

$$d[C_6H_{11}OO^*]/dt = k_2[C_6H_{11}^*][O_2] - k_3[C_6H_{11}OO^*] - k_4[C_6H_{12}][C_6H_{11}OO^*] - k_9[C_6H_{11}^*] \quad (3)$$

$$d[C_6H_{10}O]/dt = k_3[C_6H_{11}OO^*] + k_4[C_6H_{12}][C_6H_{11}OO^*] + 2k_5[C_6H_{11}^*][O_2] - k_6[C_6H_{10}O] - k_{10}[D] \quad (4)$$

$$d[C_6H_{10}OH]/dt = k_4[C_6H_{12}][C_6H_{11}OO^*] + k_7[C_6H_{11}^*][O_2] - k_8[C_6H_{10}OH] \quad (5)$$

$$d[O_2]/dt = -(k_2 + 1/2k_5)[C_6H_{11}^*][O_2] \quad (6)$$

$$d[D]/dt = k_9[C_6H_{11}^*] + k_{10}[C_6H_{10}O] \quad (7)$$

Using these equations, we carried out simulation employing Runge-Kutta 4 method (as needed for the Genetic Algorithm(GA) in this specific code for optimal curve fitting) with $\Delta t = 0.01$ min for numerically stable solution and calculated the concentrations of each component for 8 h of reaction time. The total number of iterations needed for 8-h reaction was 48,000 and the computational time required is about 5 min. In order to match the trend of the simulation results with those determined experimentally (given in Table 2) for each component, we made step 5 and step 6 of Figure 7 as reversible reactions and added two reactions (step 7 and step 8 of Figure 7) by introducing four rate constants k_6, k_8, k_9, and k_{10}. We have optimized the simulated results with the experimental values by using GA code.[60] For this, we wrote an objective function, OF (given below) as the sum of squares of the difference of simulated and experimental values of cyclohexane, cyclohexanone, and cyclohexanol.

$$OF = \alpha_1([CH]_{sim} - [CH]_{exp})^2 + \alpha_2([CHone]_{sim} - [CHone]_{exp})^2 + \alpha_3([CHol]_{sim} - [CHol]_{exp})^2 + \alpha_4([D]_{sim} - [D]_{exp})^2 \quad (8)$$

Table 3. Rate Constants at Different Temperatures Obtained by Optimization Using Genetic Algorithm

T, K	k_1, m^3/mol s	k_2, m^3/mol s	k_3, m^3/mol s	k_4, m^3/mol s	k_5, m^3/mol s	k_6, m^3/mol s	k_7, m^3/mol s	k_8, m^3/mol s	k_9, m^3/mol s	K_{10}, m^3/mol s
473	0.000419	1.36E-02	4.05E-03	1.98E-02	0.042174	7.37E-03	3.60E-03	8.27E-04	9.49E-03	6.93E-04
463	0.00003005	0.001004	0.000578	0.02579	0.00000509	0.001002	0.001624	0.000411	0.00049136	0.00012
443	0.00002033	0.001253	0.000249	0.002716	0.00000611	0.001331	0.001544	0.00038	0.00044034	0.001314
423	4.12E-04	4.71E-05	4.04E-03	1.42E-02	0.09151	5.34E-03	1.73E-03	5.45E-04	6.50E-04	5.10E-04
413	0.00006967	0.000551	0.009654	0.0026	0.0004077	0.003473	0.002044	0.000596	0.00006041	0.001068

Table 4. Arrhenius Dependence of Various Rate Constants ($K_i = A_i e^{-E/RT}$)

Rate Constant	E/R	ln A
k_1	7060.3	25.889
k_2	−6851.5	7.9995
k_3	1,2396	−34.996
k_4	−5396.6	7.4717
k_5	28,358	−73.84
k_6	6052.2	−20.029
k_7	844.2	−8.3043
k_8	1,644	−11.435
k_9	−10,924	−11.435
k_{10}	3155.8	−14.615

E, activation energy (J/mol); A, pre-exponential factor (m^3/mol s).

The GA requires a guess value of k_1 to k_{10} which is changed according to its algorithm, and in the global optimization process the cyclohexane conversion is matched first (as seen in Figure 8a) (with in about 10 iterations). If all rate constants are allowed to vary, we find that there is no convergence because of the following reason. In an attempt to match the concentrations of cyclohexanone and cyclohexanol, the rate constants k_1 and k_2 get considerably increased. Then the cyclohexane conversion increases to a very high value, this way disturbing the overall trend and giving a poor fit to the experimental data. To overcome this problem, we define OF with $\alpha_1 = 1$, $\alpha_2 = \alpha_3 = \alpha_4 = 0$ and determined optimal $k_{1op} = 4.118E\text{-}04$ cc/mol s. We have then fixed the k_1 value after matching cyclohexane conversion at this level and further carried out computations by assuming $\alpha_2 = 1$, $\alpha_1 = \alpha_3 = \alpha_4 = 0$ and varying k_2–k_{10} values. Initially, to increase cyclohexanone formation, k_3 and k_4 were increased and then to control its formation, we made the change in mechanism by making step 5 a reversible reaction and also introduced D (unidentified products), which are formed from cyclohexanone as the reaction time progresses. This reduces the simulated results of cyclohexanone formation to match with the experimental values (as in Figure 8b). In doing this way, we found that the match of the simulated cyclohexane conversion data with experimental results remained unaffected. We then fixed the values of $k_{1opt} = 4.118E\text{-}04$, $k_{2opt} = 4.708E\text{-}05$, $k_{3opt} = 4.039E\text{-}03$, $k_{5opt} = 9.151E\text{-}02$, $k_{6opt} = 5.343E\text{-}03$, $\alpha_3 = 1$, $\alpha_1 = \alpha_2 = \alpha_4 = 0$ and matched the cyclohexanol concentration (Figure 8c) by varying k_4, k_7, and k_8. The optimal values of k_4, k_7, and k_8 are $k_{4opt} = 1.417E\text{-}02$, $k_{7opt} = 1.731E\text{-}03$, and $k_{8opt} = 5.453E\text{-}04$ cc/mol s, respectively. In this process, we once again find that the match of the simulated data of conversion of cyclohexane and cyclohexanone remained unaffected. The concentrations of the intermediate species A ($C_6H_{11}^*$) and B ($C_6H_{11}OO^*$) have been plotted in Figure 8d, e and within 8 h of reaction; concentrations of A and B are far from quasi-steady state values. We have now fixed the initial guess as k_{1op} to k_{10op} for the global optimization problem and have run the genetic algorithm once again to determine optimal rate constants. The optimal results now converge with in small (less than 10) iterations and the best rate constants are reported in Table 3. We carried out similar simulations as above for different temperatures and activation energies and Arrhenious constants have been calculated and reported in Table 4.

Conclusions

In the present work, we have prepared a binuclear monometallic macrocyclic Zirconium complex and have bonded it to carbamate modified alumina to form a heterogeneous ZrZr complex catalyst. The catalyst thus prepared has been tested by FTIR Spectroscopy, UV–Vis spectroscopy, and temperature programmed desorption of ammonia. This has also been tested for its catalytic activity in the oxidation of cyclohexane at different temperatures and pressures, in which cyclohexanone was obtained as a major product, and cyclohexanol in minor quantities. The products formed by the oxidation of cyclohexane suggested that the active site in the catalyst is the ligand site and a reaction mechanism has been proposed. We further quantified the experimental results by carrying out simulations and calculated optimal rate constants at all temperatures studied using genetic algorithm. However, the pressure has negligible effect on the oxidation of cyclohexane.

Literature Cited

1. Fisher WB, Van Pepper JF. *Kirk-Othmer Encyclopedia of Chemical Technology*, 3rd ed. New York: Wiley, 1977: Vol. 7, 411–412.
2. Cuedeke VED. *Encyclopedia of Chemical Processing and Design*, Vol. 2. New York: Macel Dekker, 1977:128–132.
3. Sheu C, Richert SA, Cofre P, Ross BJ, Sobkowiak A, Sawyer DJ, Kanotsky JR. Iron-induced activation of hydrogen peroxide for the direct ketonization of methylenic carbon (cyclohexane fwdarw cyclohexanone) and the dioxygenation of acetylenes and aryl olefins. *J Am Chem Soc*. 1990;112:1936–1942.
4. Tung HC, Kang C, Sawyer DT. Nature of the reactive intermediates from the iron-induced activation of hydrogen peroxide: agents for the ketonization of methylenic carbons, the monooxygenation of hydrocarbons, and the dioxygenation of aryl olefins. *J Am Chem Soc*. 1992;114:3445–3455.
5. Traylor TG, Buyn JS, Traylor PS, Battoni P, Mansuy D. Polymeric polyhalogenated metalloporphyrin catalysts for hydroxylation of alkanes and epoxidation of alkenes. *J Am Chem Soc*. 1991;113: 7821–7823.
6. Schuchardt V, Pereira R, Rufo M. Iron(III) and copper(II) catalysed cyclohexane oxidation by molecular oxygen in the presence of *tert*-butyl hydroperoxide. *J Mol Catal A: Chem*. 1998;135:257–262.
7. Giamalva DH, Church DF, Pryor WA. Kinetics of ozonation. 6. Polycyclic aliphatic hydrocarbons. *J Org Chem*. 1988;53:3429–3432.
8. Murahashi ST, Oda Y, Naola T. Iron- and ruthenium-catalyzed oxidations of alkanes with molecular oxygen in the presence of aldehydes and acids. *J Am Chem Soc*. 1992;114:7913–7914.
9. Tolman CA, Druliner JD, Nappa MJ, Herron N.Alkane oxidation studies in DuPont's central research department. In: Hill CL,editor. Activation and Functionalization of Alkanes. New York: Wiley, 1989;317–352.
10. Perkas N, Koltyptin Y, Palchik O, Gedanken A, Chandrasekharan S. Oxidation of cyclohexane with nanostructured amorphous catalysts under mild conditions. *Appl Catal A: Gen*. 2001;209:125–130.
11. Armbruster U, Martin A, Smejkal Q, Kosslick H. Heterogeneously catalysed partial oxidation of cyclohexane in supercritical carbon dioxide. *Appl Catal A: Gen*. 2004;265:237–246.
12. Kulkarni S, Alurker M, Kumar A. Polymer support with Schiff base functional group with cobaltous palmitate as oxidation catalyst for cyclohexane. *Appl Catal A: Gen*. 1996;142:243–254.
13. Kumar A, Mishra GS, Kumar A. Oxidation of cyclohexane with molecular oxygen using a Schiff base cobalt complex bonded to carbamate-modified silica gel. *Trans Met Chem*. 2003;28:913–917.
14. Tolman CA, Druliner JD, Krusic PJ, Nappa MJ, Seidel WC, Williams ID, Ittel SD. Catalytic conversion of cyclohexylhydroperoxide to cyclohexanone and cyclohexanol. *J Mol Catal*. 1988;48:129–148.
15. Spielman M. Selectivity in hydrocarbon oxidation. *AIChE J*. 1964;10:496.
16. Alagy J, Trombouze P, Van Landeghem H. Designing a cyclohexane oxidation reactor. *Ind Eng Chem Proc Des Dev*. 1974;13:317–323.
17. Alagy J, Defoor F, Franckowiak S. *Revue de l'institut Francais du Petrile*. 1964;19:1380–1390.

18. Kharkhova TV, Arest-Yakubovich IL, Lipes VV. Kinetic model of the liquid-phase oxidation of cyclohexane. I. Homogeneous course of the process. *Kinetika Kataliz*. 1989;30:954–958 (in Russian).
19. Poherecki R, Baldyga J, Moniuk W, Podgorska W, Zdrojkowski A, Wierzchiowski PT. Kinetic model of cyclohexane oxidation. *Chem Eng Sci*. 2001;56:1285–1291.
20. Modén B, Zhan B-Z, Dakka J, Santiesteban JG, Iglesia E. Kinetics and mechanism of cyclohexane oxidation on MnAPO-5 catalysts. *J Catal*. 2006;239:390–401.
21. Loncarevic D, Cupic Z, Odovic M. Inhibition effects in the partial oxidation of cyclohexane on polymer supported Co(II) catalysts. *J Serb Chem Soc*. 2005;70:209–221.
22. Suresh AK, Sridhar T, Potter OE. Mass transfer and solubility in autocatalytic oxidation of cyclohexane. *AIChE J*. 1988;34:55–68.
23. Suresh AK, Sridhar T, Potter OE. Autocatalytic oxidation of cyclohexane—modeling reaction kinetics. *AIChE J*. 1988;34:69–80.
24. Suresh AK, Sharma MM, Sridhar T. Engineering aspects of industrial liquid-phase air oxidation of hydrocarbons. *Ind Eng Res J*. 2000;39:3958–3997.
25. Suresh AK, Sridhar T, Potter OE. Autocatalytic oxidation of cyclohexane—mass transfer and chemical reaction. *AIChE J*. 1988;34:81–93.
26. Wen Y, Potter OE, Sridhar T. Uncatalysed oxidation of cyclohexane in a continuous reactor. *Chem Eng Sci*. 1997;52:4593–4605.
27. Ponec V. Alloy catalysts: the conepts. *Appl Catal A: Gen*. 2001;222: 31–45.
28. Radecka-Paryzek W. The scandium(III) ion as a template for the synthesis of hexaaza quadridentate macrocyclic ligand. *Inorg Chim Acta*. 1979;35:349–350.
29. Radecka-Paryzek W, Patroniak-Krzyminiewska V. Azaoxa Macrocyclic and Acyclic Complexes of Lanthanides. *Collect Czech Chem Commun*. 1998;63:363–370.
30. Radecka-Paryzek W. Template synthesis and characterization of 18-membered hexaaza macrocyclic complex of lanthanum(III) perchlorate. *Inorg Chim Acta*. 1980;45:147–148.
31. Tsubomura T, Yasaku K, Sato T, Morita M. Synthesis and characterization of chiral 18-membered-macrocycle-lanthanide complexes: circular dichroism and circularly polarized luminescence. *Inorg Chem*. 1992;31:447–450.
32. Thompson LK, Mandal SK, Tandon ST, Bridson JN, Park MK. Magnetostructural correlations in bis(μ_2-phenoxide)-bridged macrocyclic dinuclear copper(II) complexes. Influence of electron-withdrawing substituents on exchange coupling. *Inorg Chem*. 1996;35: 3117–3125.
33. Spodine E, Moreno Y, Garland MT, Pena O, Baggio R. Molecular structure and magnetic properties of $[Gd(LH_4)(NO_3)_2(H_2O)]NO_3(H_2O)_2$, $[Sm(LH_4)(NO_3)_2(H_2O)]NO_3(H_2O)_{1.5}(CH_3OH)_{0.5}$ and $[Cu_2(LH_2)(H_2O)_2](NO_3)_2$ complexes (LH_4: Schiff base ligand derived from 4-methyl-2,6-diformylphenol and 1,3-diaminopropanol). *Inorg Chim Acta*. 2000;309:57–64.
34. Kuhnert N, Rossignolo GM, Periago AL. The synthesis of trianglimines: on the scope and limitations of the [3 3] cyclocondensation reaction between (1R,2R)-diaminocyclohexane and aromatic dicarboxaldehydes. *Org Biomol Chem*. 2003;1:1157–1170.
35. Na SJ, Joe DJ, Sujith S, Han W-S, Kang SO, Lee BY. Bimetallic nickel complexes of macrocyclic tetraiminodiphenols and their ethylene polymerization. *J Organomet Chem*. 2006;691:611–620.
36. Thirumavalavan M, Akilan P, Kandaswamy M. Lateral macrobicyclic compartmental mono and binuclear nickel(II) complexes derived from phenolate ligands: synthesis, spectral, electrochemical and kinetic studies. *Polyhedron*. 2005;24:1781–1791.
37. Guerriero P, Tamburini S, Vigato PA. From mononuclear to polynuclear macrocyclic or macroacyclic complexes. *Coord Chem Rev*. 1995;139:17–243.
38. Bosnich B. Cooperative bimetallic redox reactivity. *Inorg Chem*. 1999;38:2554–2562.
39. Fraser C, Johnston L, Rheingold AL, Haggerty BS, Williams CK, Whelan J, Bosnich B. Bimetallic reactivity, synthesis, structure and reactivity of homo- and heterobimetallic complexes of a binucleating macrocyclic ligand containing 6- and 4-coordination sites. *Inorg Chem*. 1992;31:1835–1844.
40. Romakh VB, Therrien B, Labat Ġl, Evans HS, Shul'pin GB, Fink GS. Dinuclear iron, ruthenium and cobalt complexes containing 1,4-dimethyl-1,4,7-triazacyclononane ligands as well as carboxylato and oxo or hydroxo bridges. *Inorg Chim Acta*. 2006;359:3294–3297.
41. Romakh VB, Therrien B, Karmazin-Brelot L, Labat Ġl, Evans HS, Shul'pin GB, Fink GS. Dinuclear iron, ruthenium and cobalt complexes containing 1,4-dimethyl-1,4,7-triazacyclononane ligands as well as carboxylato and oxo or hydroxo bridges. *Inorg Chim*. 2006; 359:1619–1626.
42. Shul'pin GB, Kudinov AR, Shul'pina LS, Petrovskaya EA. Oxidations catalyzed by osmium compounds. Part 1: Efficient alkane oxidation with peroxides catalyzed by an olefin carbonyl osmium(0) complex. *J Organomet Chem*. 2006;691:837–845.
43. Anisia KS, Mishra GS, Kumar A. Reforming of n-Hexane in presence of [1,4-bis (Salicylidene amino) phenylene] Zirconium Salen complex chemically bonded to modified Silica. *J Mol Catal A: Chem*. 2004;215:121–128.
44. Mishra GS, Kumar A. Selective Oxidation of Linear Alkanes by Schiff Base ligand 1,4-bis(salicylidene amino)-phenylene vanadium complex bonded on modified silica gel. *Kinet Catal*. 2004;45:394–399.
45. Shul'pin GB. Metal-catalysed hydrocarbon oxidations. *C R Chimie*. 2003;6:163–178.
46. Shul'pin GB, Lachter ER. Aerobic hydroxylation of hydrocarbons catalysed by vanadate ion. *J Mol Catal A: Chem*. 2003;197:65. Available at http://preprint.chemweb.com/biochem/0204001, The chemistry preprint server.
47. Gange RR, Spiro CL, Smith JJ, Hamann CA, Shiemke AK. The synthesis, redox properties, and ligand binding of heterobinuclear transition-metal macrocyclic ligand complexes. Measurement of an apparent delocalization energy in a mixed-valent copper(I)copper(II) complex. *J Am Chem Soc*. 1981;103:4073–4081.
48. Lee L-H. Adhesive Chemistry, Developments And Trends. London: Plenium Press, 1984.
49. Ryczkowski J. IR spectroscopy in catalysis. *Catal Today*. 2001; 68:263–381.
50. Finar IL. Organic Chemistry, Vol. 1: The Fundamental Principles, 6th ed., Singapore: Logman Scientific and Technical; 1973:375.
51. Mishra GS, Kumar A. Silica gel supported [1,4-bis(salicylidene amino)-phenylene] vanadium oxo complex catalyst for the oxidation of n-heptane using molecular oxygen. *J Mol Catal A: Chem*. 2003; 192:275–280.
52. Kumar A, Mishra GS, Kumar A. Covalantly bonded Schiff base cobalt complex catalyst for the selective oxidation of linear alkanes using molecular oxygen. *J Mol Catal A: Chem*. 2003;201:179–188.
53. Kishore MJL, Mishra GS, Kumar A. An alumina-supported homonuclear macrocyclic zirconium complex for reformation of n-hexane. *J Mol Catal A: Chem*. 2004;216:157–163.
54. Kishore MJL, Mishra GS, Kumar A. Synthesis of hetero binuclear macrocyclic Co-V complex bonded to chemically modified alumina support for oxidation of cyclohexane using oxygen. *J Mol Catal A: Chem*. 2005;230:35–42.
55. Yuan H-X, Xia Q-H, Zhan H-J, Lu X-H, Su K-X. Catalytic oxidation of cyclohexane to cyclohexanone and cyclohexanol by oxygen in a solvent-free system over metal-containing ZSM-5 catalysts. *Appl Catal A: Gen*. 2006;304:178–184.
56. Yao W, Chen Y, Min L, Fang H, Yan Z, Wang H, Wang J. Liquid oxidation of cyclohexane to cyclohexanol over cerium-doped MCM-41. *J Mol Catal A: Chem*. 2006;246:162–166.
57. Comon S, Parvulescu V, Grange P, Parvulescu VI. Transformation of C6 hydrocarbons over sulfated zirconia catalysts. *Appl Catal A: Gen*. 1999;176:45–62.
58. Resofszki G, Muhler M, Sprenger S, Wild U, Paál Z. Electron spectroscopy of sulfated zirconia, its activity in n-hexane conversion and possible reasons of its deactivation. *Appl Catal A: Gen*. 2003;240: 71–81.
59. Olah GA, Molnar A. *Hydrocarbon Chemistry*. New York: Wiley-Interscience; 1995:366.
60. Deb K. Optimization for Engineering Design: Algorithms and Examples. New Delhi: Prentice Hall of India; 1992.

Manuscript received July 5, 2006, and revision received Feb. 22, 2007.